RESEARCH ARTICLE

A hydrogen-bonded assembly of cucurbit[6]uril and $[MoO_2Cl_2(H_2O)_2]$ with catalytic efficacy for the one-pot conversion of olefins to alkoxy products†

Received 00th January 20xx,
Accepted 00th January 20xx

DOI: 10.1039/x0xx00000x

Lucie S. Nogueira,[a] Margarida M. Antunes,[a] Ana C. Gomes,[a] Luís Cunha-Silva,[b] Martyn Pillinger,*[a] André D. Lopes,[c] Anabela A. Valente *[a] and Isabel S. Gonçalves *[a]

The reaction of the macrocyclic cavitand cucurbit[6]uril (CB[6]) and the diaqua complex $[MoO_2Cl_2(H_2O)_2]$ in hydrochloric acid solution gave a water insoluble supramolecular compound with the general composition $2[MoO_2Cl_2(H_2O)_2]\cdot CB[6]\cdot xH_2O\cdot yHCl\cdot z(CH_3COCH_3)$ (**2**). Single crystal X-ray diffraction (XRD) analysis revealed the presence of barrel-shape supramolecular entities, $\{CB[6]\cdot 10(H_2O)\}$, aligned in layers which are shifted relative to adjacent layers to form a brick-like pattern. The CB[6]/water hydrogen-bonded entities further engage in intermolecular interactions with water, HCl and $[MoO_2Cl_2(H_2O)_2]$ molecules to form a three-dimensional (3D) framework. Compound **2** was characterised by thermogravimetric analysis (TGA), IR and Raman vibrational spectroscopy, and $^{13}C\{^1H\}$ CP MAS NMR. The reference complex $[MoO_2Cl_2(H_2O)_2]\cdot(diglyme)_2$ (**1**) and compound **2** were studied for the oxidative catalytic conversion of olefins (*cis*-cyclooctene, cyclohexene and styrene) with aqueous H_2O_2 as oxidant. Using alcohols as solvents, **2** was employed in a one-pot two-stage strategy for converting olefins to alkoxy products, which involves oxidation (with H_2O_2) and acid chemistry. Mechanistic studies were carried out using different intermediates as substrates, and the type of solvent and substrate scope were investigated. The results demonstrated the ability of the CB[6]/Mo^{VI} supramolecular adduct to function as an acid-oxidation multifunctional catalyst, and its recovery and reuse via relatively simple procedures.

Introduction

Molybdenum(VI) dichloride dioxide, MoO_2Cl_2, was first reported by Berzelius in 1826, and is generally believed to be the first molybdenum oxo compound.[1] MoO_2Cl_2 is a very useful starting material for synthesising a variety of molybdenum compounds and has gained importance as a catalyst in organic transformations.[2] Anhydrous MoO_2Cl_2 has a layered structure in the solid-state consisting of infinite chains (···O=Mo···O=Mo···) in two directions, with the Cl atoms occupying the apical positions of distorted $\{MoO_4Cl_2\}$ octahedra.[3] Although MoO_2Cl_2 is moisture sensitive, monohydrate and dihydrate derivatives are known. In $MoO_2Cl_2\cdot H_2O$, the introduction of a water molecule into the coordination sphere of Mo atoms breaks down the layers into chains in which one of the oxygen atoms is terminal and the other is bridging.[4] When two H_2O molecules are coordinated to the Mo atom, the structure consists of isolated $[MoO_2Cl_2(H_2O)_2]$ molecules.

The neutral species $[MoO_2Cl_2(H_2O)_2]$ exists in solutions of alkali molybdates in concentrated hydrochloric acid and can be extracted with oxygenated organic solvents such as diethyl ether.[5] Two main avenues have been pursued to isolate air-stable crystalline solids containing the diaqua complex: 1) adduct formation with polyethers such as diglyme[6] or crown ethers such as 18-crown-6[7]; 2) co-crystallisation with ammonium ions such as pyridinium,[8] triethylammonium,[9] 1,3-bis(4-pyridinium)propane (H_2dipy-pra)[10] and 2,2'-dipyridylammonium (Hdpa)[11] (all with chloride as the counterion). These compounds display intricate hydrogen-bonding networks that give rise to supramolecular frameworks. The 2D network material $[MoO_2Cl_2(H_2O)_2]\cdot(H_2dipy\text{-}pra)Cl_2$ was found to be an efficient catalyst, with H_2O_2 as the oxidant and $NaHCO_3$ as the cocatalyst, in the epoxidation of olefins.[10] Later, Costa *et al.* reported that the 3D framework material $[MoO_2Cl_2(H_2O)_2]\cdot Hdpa\cdot Cl\cdot H_2O$ was an effective catalyst (without any cocatalyst added such as $NaHCO_3$) for the H_2O_2-mediated epoxidation of cyclooctene.[11]

In the present paper, a new supramolecular approach to the solid-state isolation of $[MoO_2Cl_2(H_2O)_2]$ is reported, using the macrocyclic cavitand cucurbit[6]uril (CB[6]). Cucurbit[*n*]urils (CB[*n* = 5-8, 10, 14]) are composed of *n* glycoluril units lined by 2*n* methylene bridges to form a hydrophobic cavity accessible through two carbonyl-lined portals.[12] CBs can interact with metal complexes to form either host-guest inclusion

[a] Department of Chemistry, CICECO - Aveiro Institute of Materials, University of Aveiro, Campus Universitário de Santiago, 3810-193 Aveiro, Portugal. E-mail: mpillinger@ua.pt (M.P.), atav@ua.pt (A.A.V.), igoncalves@ua.pt (I.S.G.)
[b] REQUIMTE/LAQV & Department of Chemistry and Biochemistry, Faculty of Sciences, University of Porto, 4169-007 Porto, Portugal.
[c] CCMar, and Department of Chemistry and Pharmacy, FCT, University of the Algarve, P-8005-039 Faro, Portugal.

† Electronic Supplementary Information (ESI) available: Materials and methods experimental details, synthesis of CB[6], XRD experimental details and geometrical data for H-bonding interactions in **2**, experimental and simulated PXRD patterns for **2**, TGA curves, ATR FT-IR, PXRD and SEM results for recovered catalysts, mass spectral data for selected products. CCDC 1900402. For ESI and crystallographic data in CIF or other electronic format see DOI: 10.1039/x0xx00000x

compounds, in which the CB acts as a molecular container,[12] or outer-sphere exclusion complexes, in which the CO groups coordinate either directly or indirectly with metal ions, complexes or clusters.[13] Fedin and co-workers have made the largest contribution to CB[*n*]-based coordination chemistry with metal cations.[14] In aqueous solution, transition-metal aqua complexes generally interact with CBs indirectly via hydrogen bonds between the coordinated water molecules and the portal oxygen atoms of the CB. This gives rise to supramolecular adducts which crystallise with complex network structures, such as that found with CB[6] and the trinuclear molybdenum oxo cluster $[Mo_3O_4(H_2O)_6Cl_3]^+$.[14c]

Although CB[6] is virtually insoluble in water, it is soluble in acidic aqueous solution. Fedin and co-workers were successful in isolating poorly soluble CB[6] coordination complexes by pairing the cavitand with metal complexes that were stable in HCl solution, such as the trinuclear molybdenum complex mentioned above. We have now used an analogous strategy to isolate a supramolecular adduct from a HCl solution containing CB[6] and $[MoO_2Cl_2(H_2O)_2]$. The crystal structure of the adduct consists of a 3D hydrogen-bonding framework built from assemblies of CB[6] and the diaqua complex in a net ratio of 1:2. Encouraged by the catalytic results reported previously for adducts containing the diaqua complex, the utility of the CB[6] adduct in catalysed organic reactions, namely oxidation (the epoxidation of olefins) and oxidation/acid catalysis (the one-pot conversion of olefins with aqueous H_2O_2 to alkoxy ketone and alcohol products) has been investigated. The catalyst stability was studied and mechanistic insights were obtained by using different types of intermediates as substrates.

Results and Discussion

Synthesis and characterisation of supramolecular adduct $2[MoO_2Cl_2(H_2O)_2]\cdot(C_{36}H_{36}N_{24}O_{12})\cdot xH_2O\cdot yHCl\cdot z(CH_3COCH_3)$ (2)

The supramolecular adduct **2** precipitated after mixing an aqueous solution of $[MoO_2Cl_2(H_2O)_2]$ (prepared by dissolving MoO_3 in 6 M HCl) with a hydrochloric acid solution of CB[6]. Prolonged standing of the mother liquor at ambient temperature led to the formation of pale yellow single crystals suitable for structure determination by XRD.

According to the XRD study, compound **2** is a supramolecular adduct of a CB[6] molecule and two $[MoO_2Cl_2(H_2O)_2]$ complexes (Fig. 1), with a high number of water molecules of crystallisation and HCl, ultimately formulated as $2[MoO_2Cl_2(H_2O)_2]\cdot(C_{36}H_{36}N_{24}O_{12})\cdot 17H_2O\cdot 2HCl$. The crystal structure was solved in the centrosymmetric triclinic space group *P*-1 with the asymmetric unit (asu) containing one neutral complex $[MoO_2Cl_2(H_2O)_2]$, one half of a CB[6] molecule, and several solvent molecules (8.5 H_2O molecules of crystallisation and one HCl molecule; the CB[6] cavity is occupied by H_2O molecules, with the crystal refined model pointing to 2.5 molecules occupying six potential sites). The most important structural features of the $\{MoO_4Cl_2\}$ centre of the inorganic complex in **2** are consistent with those observed in the previous crystal structures containing this complex, reported in the Cambridge Structural Database (version 5.39 – 2018)[15,16]: CSD codes YEYWOO,[6] FEKCED,[7a] FEKCED01,[7b] KEQBUE,[7b] XMOPYC10,[8] LAPPOH,[9] KICNIU,[10] MUPGIO,[11] and VONXUS.[17] The Mo^{VI} coordination centre displays a distorted octahedral geometry, with the four O-atoms (two oxido groups, Mo=O, and two water molecules, Mo–Ow) in the basal plane, and two chlorine atoms, Mo–Cl, occupying the axial positions (Fig. 1; Table 1 gives details about the coordination bond lengths and internal angles).

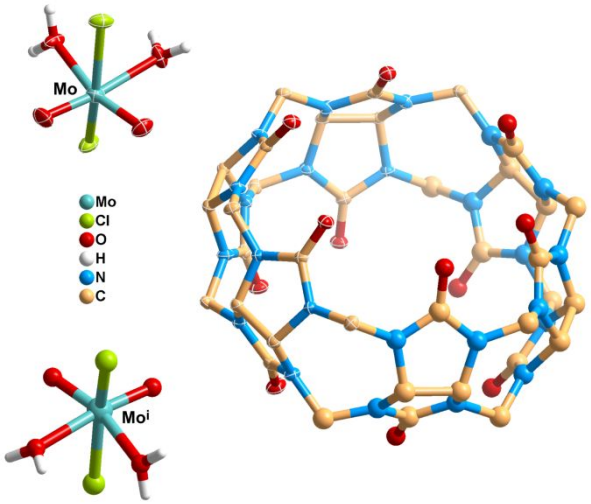

Fig. 1 Crystal structure of the supramolecular adduct of $[MoO_2Cl_2(H_2O)_2]$ and CB[6] (**2**). Non-H atoms of the asu are represented as ellipsoids with thermal displacement at the 50% probability level, while those generated by symmetry are drawn in ball-and-stick mode, and most of the H-atoms are omitted for clarity (symmetry transformation used to generate equivalent atoms: (i) *–x, 2–y, 1–z*).

The extended crystal structure of the adduct **2** reveals a supramolecular assembly of metal complexes with CB[6]. Since the Mo complex is not incorporated into the hydrophobic cavity of CB[6], it can be envisaged as an exclusion complex or, alternatively, as a lattice exclusion compound (Fig. 2).[18] The structural cohesion of this novel adduct is guaranteed by an extensive network of intermolecular interactions, mainly strong O–H···O and C–H···Cl hydrogen bonds, intermediated by numerous H_2O molecules of crystallisation and HCl molecules. Interestingly, five carbonyl groups of each CB[6] rim interact with five H_2O molecules by O–H···O hydrogen bonds, leading to the formation of barrel-shape supramolecular entities, $\{CB[6]\cdot 10(H_2O)\}$ (Fig. 2a; geometric information concerning all the strong hydrogen bonds are detailed in Table S2 in the ESI†). These barrel-shape supramolecular entities are involved in further contacts with the remaining H_2O molecules of crystallisation and HCl molecules, as well as with the complex $[MoO_2Cl_2(H_2O)_2]$, leading to the formation of a 3D hydrogen-bonded framework (Fig. 2b and 2c). The occurrence of a high number of H_2O molecules of crystallisation and, consequently, the extensive network of strong intermolecular interactions is crucial in reinforcing the cohesion of the crystalline structure.

The bulk powder obtained in the reaction for **2** was further characterised by elemental analysis, powder XRD (PXRD), N_2 adsorption at 196 °C, TGA, and the spectroscopic techniques FT-IR, FT-Raman and $^{13}C\{^1H\}$ CP MAS NMR. Fig. S1 in the ESI†

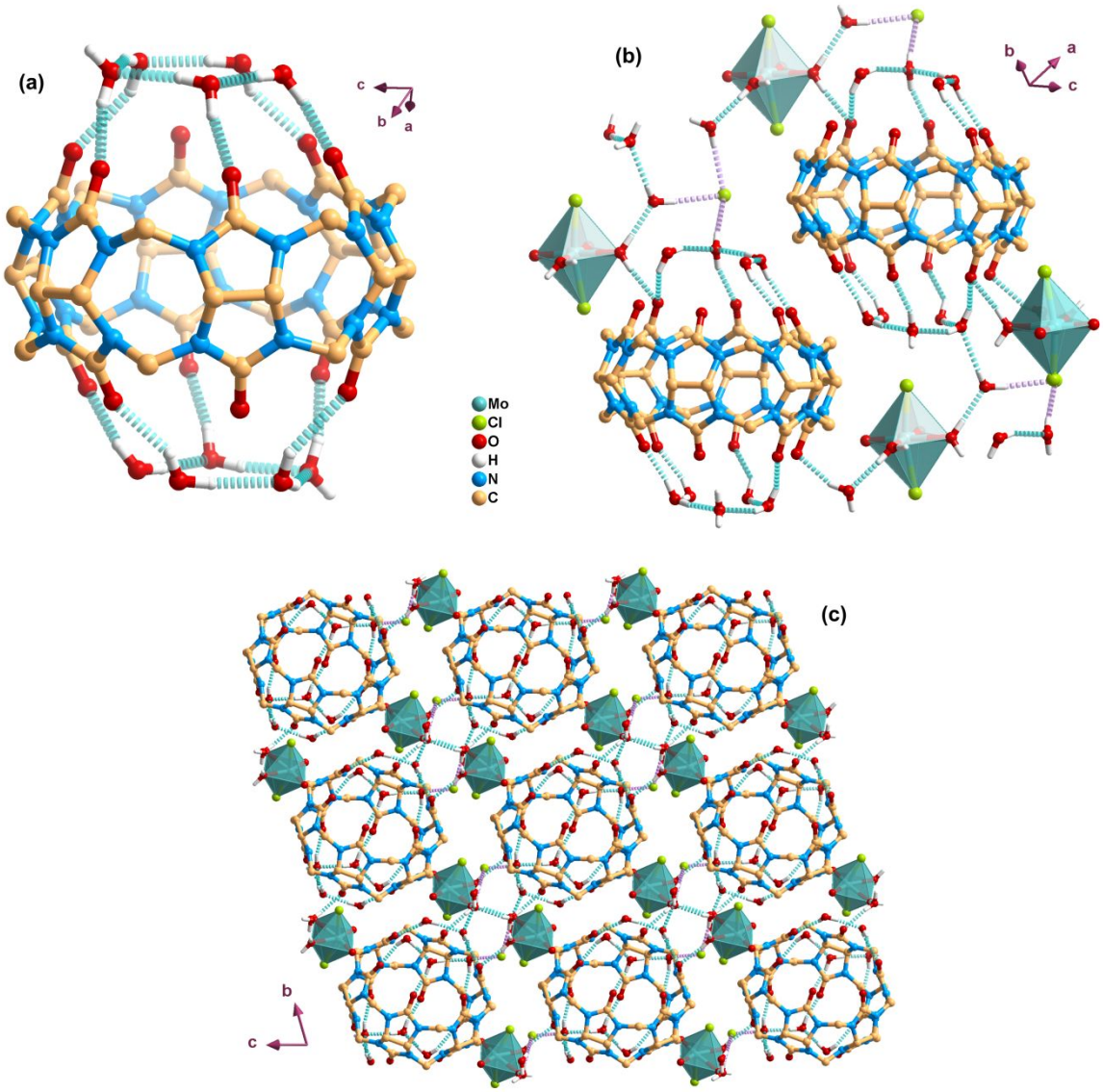

Fig. 2 Selected features in the crystal structure of the supramolecular adduct of $[MoO_2Cl_2(H_2O)_2]$ and CB[6] (**2**): (a) barrel-shape supramolecular entity {CB[6]·10(H_2O)}; (b) O–H···O and O–H···Cl interactions between adjacent neutral Mo complexes and CB[6] molecules, intermediated by water and HCl molecules; (c) overall crystalline arrangement viewed along the [1 0 0] direction of the unit cell. O–H···O and O–H···Cl interactions are represented as blue and pink dashed lines, respectively.

compares the observed PXRD pattern of the bulk microcrystalline sample of **2** with a simulated pattern based on the single crystal structure data. The good match between the two patterns proves that the powder had the same crystalline structure with a high degree of phase purity. Elemental analysis of the powder indicated the composition $2[MoO_2Cl_2(H_2O)_2]\cdot(C_{36}H_{36}N_{24}O_{12})\cdot 15H_2O\cdot 1.5HCl \cdot 0.6(CH_3COCH_3)$, which is similar to that determined by X-ray crystallography except for minor differences in the water and HCl contents, and the presence of acetone. The presence of acetone (originating from the CB[6] starting material) was confirmed by $^{13}C\{^1H\}$ CP MAS NMR, while the water content was supported by TGA measurements which revealed a mass loss step of 20.6% up to 150 °C attributed to the removal of water and acetone (Fig. S2 in the ESI†). Acetone was not detected by X-ray crystallography, possibly because of disorder. The TGA profiles of the starting material CB[6] and compound **2** show that the organic cavitand starts to decompose around 290 °C. Two overlapping steps are clearly visible for **2**, a slightly prolonged one with a derivative thermogravimetric (DTG) maximum at 330 °C, followed by a more abrupt loss with DTG_{max} = 390 °C. For comparison, the DTG_{max} value for CB[6] is 400 °C. Decomposition of the organic matter in **2** is complete at 500 °C, leaving residual MoO_3 (12.0%), which starts to sublime above 700 °C.

The N_2 adsorption-desorption isotherm for **2** at -196 °C was of type II, which may be associated with monolayer-multilayer adsorption on an essentially non-porous material. The specific surface area was 9 $m^2\ g^{-1}$. The inner cavity diameter of CB[6] is ca. 0.39 nm which is slightly greater than that of the N_2 molecule (ca. 0.36 nm), but the accessibility of the adsorbate molecules to the cavities seems to be hindered in the crystal structure of

2. The pore size distribution was centred at ca. 2.8 nm which may be associated with intercrystallite void spaces. One cannot exclude the possibility of the surface area changing upon dispersion of the solid in a liquid phase (in this work, the catalytic tests are biphasic solid-liquid) partly due to interfacial interactions between the two phases.

The FT-IR and FT-Raman spectra of **2** are dominated by the characteristic bands of CB[6] (Fig. 3). Nevertheless, a few additional bands are present that can be assigned to the incorporated molybdenum complex: (IR, cm^{-1}) 334 (ν_{asym}(Mo–Cl)), 915 (ν_{asym}(Mo=O)); (Raman, cm^{-1}) 252 (ρ(MoO_2)), 310 (ν_{sym}(Mo–Cl)), 920 (ν_{asym}(Mo=O)), 960 (ν_{sym}(Mo=O)).[7a] The reference complex $[MoO_2Cl_2(H_2O)_2]\cdot(diglyme)_2$ (**1**)[6] displays bands at near-identical frequencies: (IR) 334, 914 and 953 cm^{-1}; (Raman) 252, 315, 920 and 951 cm^{-1}.

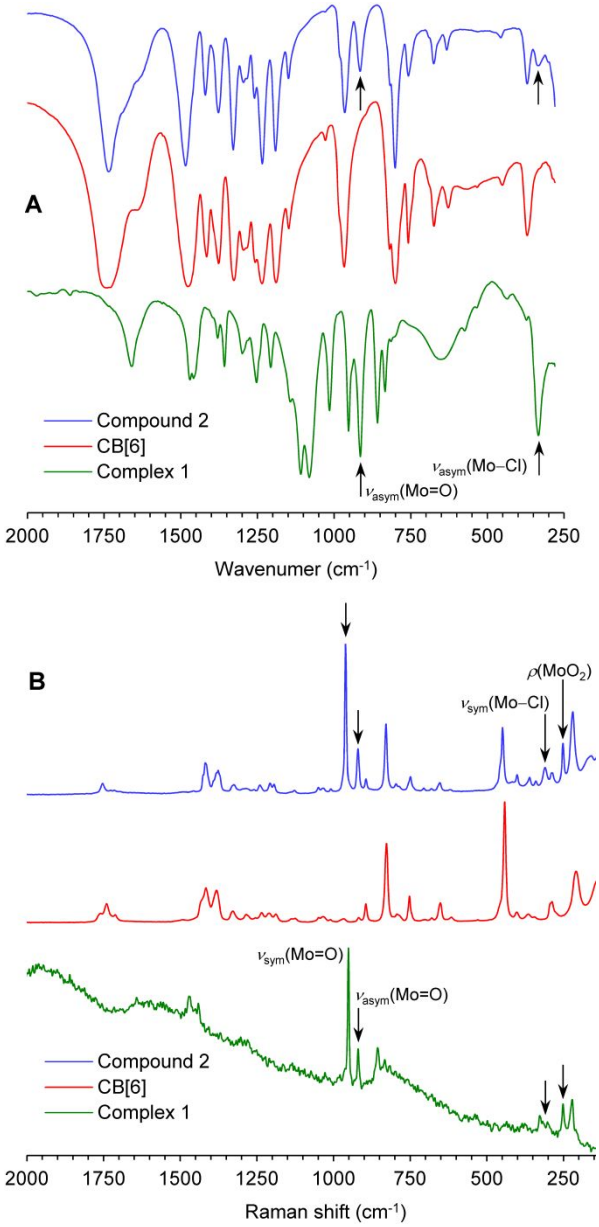

Fig. 3 FT-IR (A) and Raman (B) spectra of complex **1**, CB[6] and compound **2**.

Table 1 Selected bond lengths (Å) and angles (°) for the Mo^{VI} coordination centre of the neutral complex $[MoO_2Cl_2(H_2O)_2]$ in the crystal structure of **2**

Mo1–O1	1.6779(15)	Mo1–O2W	2.2750(14)
Mo1–O2	1.6859(14)	Mo1–Cl2	2.3672(5)
Mo1–O1W	2.2231(14)	Mo1–Cl1	2.3804(5)
O1–Mo1–O2	103.55(8)	O2–Mo1–Cl1	97.11(5)
O1–Mo1–O1W	95.01(7)	O1W–Mo1–O2W	77.22(6)
O1–Mo1–O2W	172.23(7)	O1W–Mo1–Cl2	79.56(4)
O1–Mo1–Cl2	96.12(6)	O1W–Mo1–Cl1	81.52(4)
O1–Mo1–Cl1	95.48(6)	O2W–Mo1–Cl2	82.95(4)
O2–Mo1–O1W	161.42(7)	O2W–Mo1–Cl1	83.12(4)
O2–Mo1–O2W	84.21(6)	Cl2–Mo1–Cl1	158.563(19)
O2–Mo1–Cl2	97.61(5)		

$^{13}C\{^1H\}$ CP MAS NMR spectra for CB[6] and **2** are shown in Fig. 4. The spectrum for CB[6] shows three somewhat broad and featureless signals at 155.5, 70.5 and 52.0 ppm for the three chemically distinct carbon types (C=O, C–H and bridging CH_2, respectively). The spectrum for **2** is slightly different in that each of the three resonances is split, showing between two and three resolved lines. This can be attributed to the fact that the crystallographically inequivalent carbons for each type of carbon functionality (i.e., six CO groups, six C–H and six CH_2) may have slightly different environments and therefore small differences in chemical shift, which can result in the observation of multiple sharp resonances for one chemically distinct carbon type.

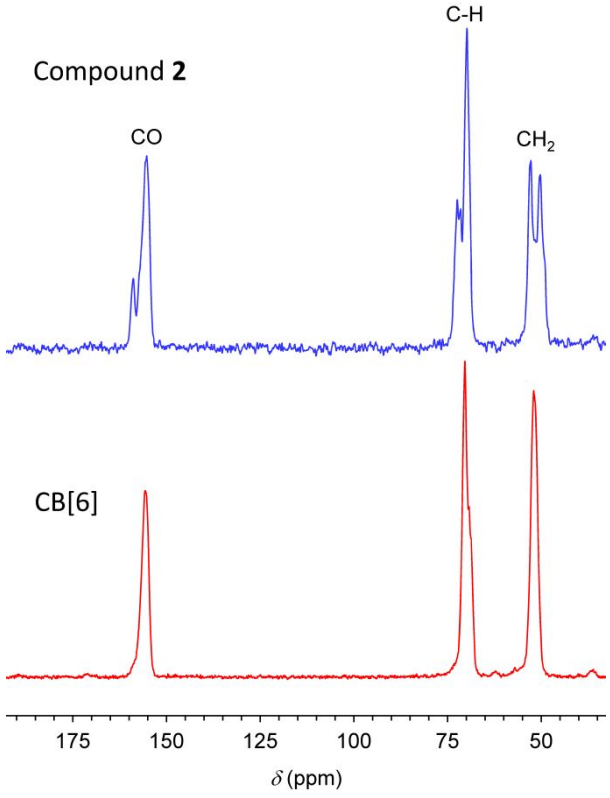

Fig. 4 $^{13}C\{^1H\}$ CP MAS NMR spectra for CB[6] and the supramolecular adduct **2**.

Catalytic studies

Olefins, which may derive from fossil or renewable sources, can be converted to many useful products such as epoxides, 1,2-alkoxy alcohols and 1,2-alkoxy ketones.[19] Hydrogen peroxide is an attractive oxidant for catalytic olefin epoxidation due to its relatively low cost and eco-friendliness, giving water as the coproduct from its consumption.[20] Epoxides are versatile intermediates for various organic reactions with, for example, nucleophiles, acids, bases, reducing and oxidizing agents.[19] In particular, epoxides may be converted in alcohol media to 1,2-disubstituted products (which usually have a *trans* configuration), such as 1,2-alkoxy alcohols and 1,2-alkoxy ketones, which have important applications as intermediates in the pharmaceutical sector.[21] For example, *trans*-2-methoxycyclohexanol is a key intermediate for the synthesis of tricyclic beta-lactam antibiotics.[21c] On the other hand, the conversion of olefins in alcohol medium to alkoxy products is a useful tool in organic synthesis for improving product selectivity by enabling protective group formation.[22] With these considerations in mind, we studied the catalytic ability of **2** in two stages, firstly to assess its performance for the epoxidation of olefins with H_2O_2, and secondly to apply this catalytic efficacy in the one-pot conversion of olefins to alkoxy ketone and alcohol products.

Olefin epoxidation

The catalytic properties of **2** were explored starting with *cis*-cyclooctene (Cy_8) as a model substrate, which is often used in the literature for catalyst benchmarking of molybdenum compounds bearing the $\{MoO_2Cl_2\}$ moiety in olefin epoxidation with hydroperoxide oxidants. The reaction of Cy_8 with H_2O_2 at 70 °C in the presence of **2**, using acetonitrile as solvent, led to 100% epoxide (Cy_8O) selectivity at 85% conversion (Scheme 1, Table 2). Pristine CB[6] led to a sluggish reaction of Cy_8 (7-10% conversion), suggesting that the epoxidation reaction with **2** involved molybdenum-containing active species. The results for the model complex $[MoO_2Cl_2(H_2O)_2]\cdot(diglyme)_2$ (**1**) (100% Cy_8O selectivity at 93% conversion) are comparable with those for **2**. An important difference between compounds **1** and **2** is that the former was completely soluble in the reaction medium and therefore difficult to separate, whereas **2** could be recovered and reused in consecutive batch runs (discussed below). Decreasing the reaction temperature from 70 to 55 °C led to slower kinetics in the presence of **2** (100% Cy_8O selectivity at 73% conversion), as did the use of *N*,*N*′-dimethylformamide (DMF) as solvent instead of MeCN (100% Cy_8O selectivity at 28% conversion). These results may be partly due to the stronger basicity of DMF than MeCN, which may lead to competitive effects between solvent and reactant molecules in the coordination to the (Lewis acid) metal centre.[23] Without a solvent or using water, the reaction was very sluggish (≤ 2% Cy_8 conversion at 24 h). Water is less basic than MeCN, suggesting that non-protic polar solvents of moderate basicity may be favourable.

There are relatively few reports on catalytic olefin epoxidation with H_2O_2 as the oxygen source and complexes of the type $[MoO_2Cl_2(L)_n]$ as the catalyst source. With the 2D network material $[MoO_2Cl_2(H_2O)_2]\cdot(H_2dipy\text{-}pra)Cl_2$ as the catalyst (1 mol%), $NaHCO_3$ as cocatalyst (25 mol%) and MeCN as solvent, Wang and co-workers obtained a high Cy_8O yield of 99% after 1 h at 25 °C.[10] Under conditions more similar to those used in the present work (no $NaHCO_3$ cocatalyst), the 3D framework material $[MoO_2Cl_2(H_2O)_2]\cdot Hdpa\cdot Cl\cdot H_2O$ led to a Cy_8O yield of 80% after 24 h at 50 °C,[11] which is comparable with the catalytic performance measured for **2**.

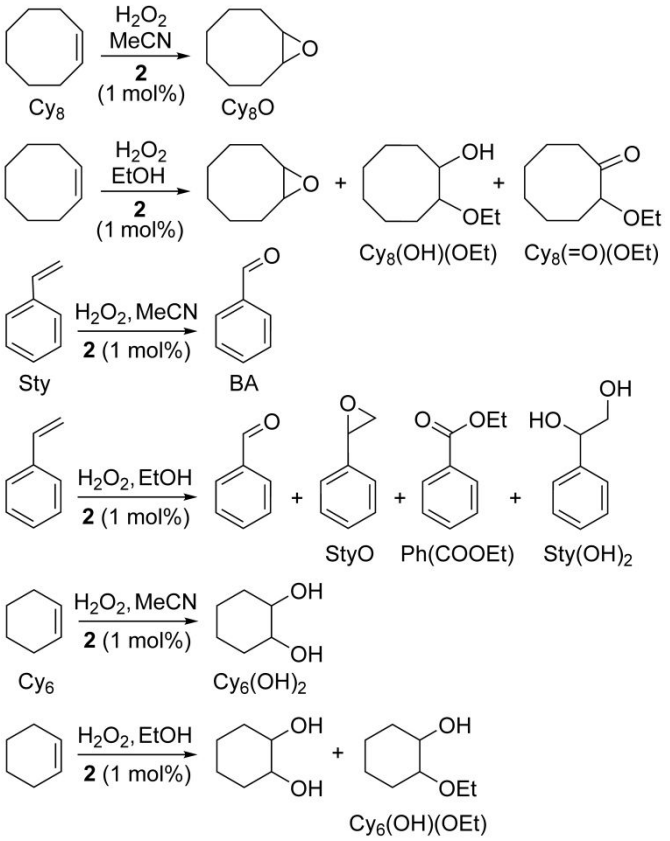

Scheme 1 Products obtained in the oxidation of *cis*-cyclooctene, styrene and cyclohexene with H_2O_2 in the presence of **2**, using MeCN or EtOH as solvent.

Table 2 Oxidation of olefins with H_2O_2 in the presence of compounds **1**, **2** and CB[6][a]

Catalyst	Substrate	Product	*T* (°C)	Solvent	Conversion (%)
1	Cy_8	Cy_8O	70	MeCN	93
2			55	MeCN	73
2			70	MeCN	85
2			70	DMF	28
2			70	none	2
2			70	H_2O	1
CB[6]			70	MeCN	10
2	Cy_6	$Cy_6(OH)_2$	70	MeCN	42
2	Sty	BA	70	MeCN	47

[a] Reaction conditions: Molar ratio Mo:substrate:H_2O_2 = 1:100:152, 24 h reaction. The selectivity to the indicated product was 100% in all cases.

Compound **2** was effective for the catalytic conversion of other industrially produced alkenes, namely styrene (Sty) and cyclohexene (Cy_6), which were chosen as representative aromatic and aliphatic substrates (Table 2, Scheme 1). There are

several reports of the oxidation of styrene or cyclohexene catalysed by dioxomolybdenum(VI) complexes, where H_2O_2 has been used as an oxidant.[24] In many cases, especially for styrene, aqueous 30% H_2O_2 as the sole oxidant gives poor catalytic efficiency, with low styrene oxide (StyO) selectivity, whereas the addition of the cocatalyst $NaHCO_3$ activates the catalytic oxidation process and leads to much higher StyO selectivity.[20b,25] The results obtained in the present work (without a cocatalyst) are consistent with these observations. Thus, the oxidation of Sty at 70 °C gave benzaldehyde (BA) with 100% selectivity at 47% conversion (24 h). According to literature studies on the mechanism of Sty oxidation, StyO is an intermediate to BA, and the latter may be formed via nucleophilic attack of H_2O_2 on StyO giving a hydroxyl-hydroperoxy intermediate followed by oxidative cleavage,[26-28] or BA may be formed via the direct oxidative cleavage of the side chain C=C double bond of Sty via a radical mechanism (Scheme 2).[26,27,29] The initial addition of a radical scavenger (2,6-di-tert-butyl-4-methyl phenol) to the catalytic reaction mixture, in an equimolar amount relative to the substrate, strongly affected the reaction kinetics (2% conversion compared to 60% conversion without radical scavenger). These results suggest the predominance of a radical mechanism. The reaction of Cy_6 with H_2O_2 in the presence of **2** gave cyclohexanediol ($Cy_6(OH)_2$) in 100% selectivity at 42% conversion (Scheme 1). The diol may be formed via the intermediate formation of cyclohexene oxide (Cy_6O),[30] as suggested in Scheme 2 for StyO.

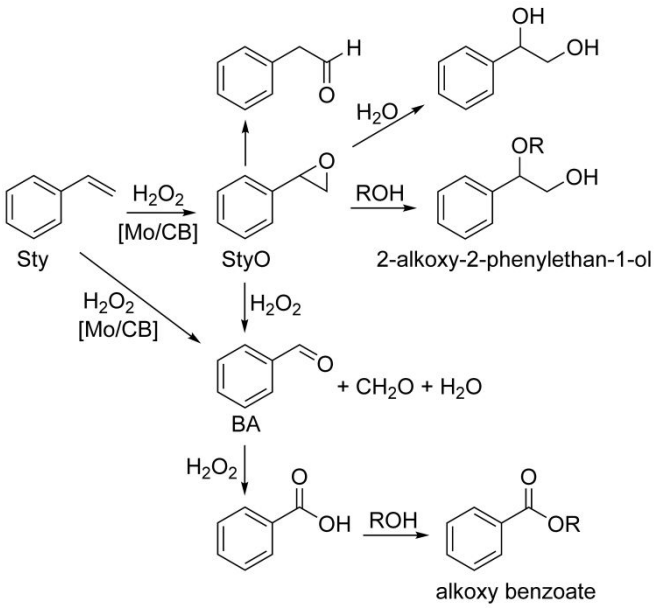

Scheme 2 Possible products of the oxidation reaction of styrene with H_2O_2.[26,27,29]

One-pot conversion of *cis*-cyclooctene to alkoxy products

Compound **2** was tested as a multifunctional catalyst for the integrated conversion of olefins to alkoxy products in alcohol media. These reaction systems involve oxidation and acid chemistry. The one-pot conversion was carried out in two stages (24 h reaction at 70 °C followed by 24 h reaction at 90 °C) with the objective of enhancing selectivity to the intermediates in the first stage (involving oxidation catalysis), followed by conversion of the intermediates to the alkoxy products in the second stage (involving acid catalysis). Catalyst **2** was tested first with Cy_8 as model substrate.

Table 3 Catalytic results for the oxidation of cyclooctyl substrates with H_2O_2 in the presence of **2** using an alcohol as solvent[a]

Ent.	Cat.	Sub.	Product	*T* (°C)	*t* (h)	Solvent	Conv. (%)	Sel. (%)
1	**1**	Cy_8	Cy_8O	70	24	EtOH	91	83
			$Cy_8(OH)(OEt)$					7
			$Cy_8(=O)(OEt)$					10
2		Cy_8	Cy_8O	90[b]	48	EtOH	92	32
			$Cy_8(OH)(OEt)$					31
			$Cy_8(=O)(OEt)$					33
			$Cy_8(OH)_2$					4
3	**2**	Cy_8	Cy_8O	70	24	MeOH	80	> 99
			$Cy_8(OH)(OMe)$					<1
4		Cy_8	Cy_8O	90[b]	48	MeOH	82	51
			$Cy_8(OH)(OMe)$					46
			$Cy_8(OMe)_2$					3
5		Cy_8	Cy_8O	70	24	EtOH	89	90
			$Cy_8(OH)(OEt)$					3
			$Cy_8(=O)(OEt)$					6
6		Cy_8	Cy_8O	90[b]	48	EtOH	90	57
			$Cy_8(OH)(OEt)$					18
			$Cy_8(=O)(OEt)$					26
7		Cy_8	Cy_8O	70	24	BuOH	90	93
			$Cy_8(OH)(OBu)$					2
			$Cy_8(=O)(OBu)$					5
8		Cy_8	Cy_8O	90[b]	48	BuOH	90	64
			$Cy_8(OH)(OBu)$					10
			$Cy_8(=O)(OBu)$					27
9	**1**	Cy_8O	$Cy_8(OH)(OEt)$	70	24	EtOH	22	55
			$Cy_8(=O)(OEt)$					45
10		Cy_8O	$Cy_8(OH)(OEt)$	90	24	EtOH	71	43
			$Cy_8(=O)(OEt)$					58
11	**2**	Cy_8O	$Cy_8(OH)(OEt)$	70	24	EtOH	12	52
			$Cy_8(=O)(OEt)$					48
12	none	Cy_8O	$Cy_8(OH)(OEt)$	70	24	EtOH	0	0
			$Cy_8(=O)(OEt)$					
13	**2**	$Cy_8(OH)$	$Cy_8(=O)$	70	24	EtOH	50	100
14	none	$Cy_8(OH)$	$Cy_8(=O)$	70	24	EtOH	14	100
15	**2**	$Cy_8(OH)_2$	$Cy_8(OH)(OEt)$	70	24	EtOH	100	5
			$Cy_8(=O)(OEt)$					52
			$Cy_8(=O)OH$					28
			$Cy_8(=O)_2$					15
16	none	$Cy_8(OH)_2$	$Cy_8(OH)(OEt)$	70	24	EtOH	99	8
			$Cy_8(=O)(OEt)$					91
			$Cy_8(=O)OH$					0
			$Cy_8(=O)_2$					0
17	CB[6]	Cy_8	Cy_8O	70	24	EtOH	6	100
18		Cy_8	Cy_8O	90[b]	48	EtOH	25	100
19		Cy_8O	$Cy_8(OH)(OEt)$	70	24	EtOH	0	0
			$Cy_8(=O)(OEt)$					
20		Cy_8O	$Cy_8(OH)(OEt)$	90	24	EtOH	2	78
			$Cy_8(=O)(OEt)$					22

[a] Reaction conditions: Molar ratio Mo:substrate:H_2O_2 = 1:100:152. Ent. = Entry; Cat. = Catalyst; Sub. = Substrate; Conv. = Conversion; Sel. = Selectivity. [b] First 24 h at 70 °C.

The one-pot first-stage process of **2**/Cy_8/H_2O_2/ethanol led to high epoxide selectivity of 90% at 89% conversion, and the products 2-ethoxycyclooctanol [Cy_8(OH)(OEt)] and 2-ethoxycyclooctanone [Cy_8(=O)(OEt)] were formed in low yields of 3% and 5%, respectively (Table 3, entry 5). Using methanol (MeOH) or 1-butanol (BuOH) as solvent led to high epoxide selectivity (93-99%) at high conversion (80-90%), and the alkoxy products were formed (for BuOH), albeit in low yields, at 70 °C (entries 3 and 7). BuOH and EtOH led to higher Cy_8 conversions than MeOH.

In the one-pot two-stage process in the different alcohol media, **2** led to epoxide yields of 42-58% and relatively high yields of alkoxy products (33-40% total yield at 48 h) (Table 3). The reaction in MeOH was slowest. The epoxide yield decreased and the total yield of alkoxy products increased in the order: BuOH → EtOH → MeOH (entries 8, 6 and 4, respectively). The differences in kinetics may be partly due to differences in nucleophilicity of the alcohols. For example, since EtOH is a stronger nucleophile than MeOH, the formation of the respective alkoxy products (via alcoholysis) may be faster (8% (entry 5) compared to <1% (entry 3) at 24 h), driving the epoxidation step forward and thus increasing Cy_8 conversion (compared to the reaction using MeOH).

In the one-pot two-stage process with ethanol as solvent, pristine CB[6] gave a sluggish reaction (ca. 25% conversion at 48 h, Table 3, entry 18). The model complex **1** led to 92% conversion and a total yield of 59% for Cy_8(OH)(OEt) and Cy_8(=O)(OEt) (entry 2), which represents similar performance to that obtained with **2** (90% conversion, 40% yield of alkoxy products, entry 6). However, as mentioned above, complex **1** has different solubility characteristics compared to **2**, which has a major impact on catalyst recovery processes.

Mechanistic insights

To gain mechanistic insights into these reaction systems, **2** was tested with cyclooctyl substrates at 70 °C using H_2O_2/EtOH (Table 3). The choices of the substrates were based on the possibility of them being intermediates in the overall reaction, or to check the ability of the catalyst to perform specific types of chemical transformations. Based on these studies, an overall mechanistic proposal is presented in Scheme 3. Specifically, catalyst **2** with the epoxide Cy_8O as substrate led to Cy_8(OH)(OEt) and Cy_8(=O)(OEt), formed in ca. 6% yield each at 12% conversion (24 h) (Table 3, entry 11). These results, taken together with those for the one-pot two-stage process, indicate that the alkoxy products are formed via the intermediate formation of the epoxide (path A in Scheme 3), with this consecutive step being favoured at higher temperature (in the second stage at 90 °C, entry 5 in Table 3). The epoxide ring-opening step may be promoted by Lewis acidity associated with the molybdenum centre or Brønsted acidity associated with the cucurbituril component of **2**. Control tests with Cy_8O as substrate in the presence of CB[6] or **1** (70 °C, 24 h) indicated that the ring-opening reaction did not occur in the presence of the cucurbituril component (CB[6] led to 0% conversion, entry 19 in Table 3), whereas the molybdenum compound **1** presented some activity (22% conversion, 100% selectivity to alkoxy products, entry 9). For a better understanding, the reaction of Cy_8O was further tested at 90 °C for 24 h. Under these conditions, **1** led to 71% conversion (entry 10) and CB[6] led to a sluggish Cy_8O reaction (2% conversion, entry 20). Hence, the active species involved in the formation of the alkoxy products may essentially be of Lewis acid type.

The alkoxy alcohol may be converted to the corresponding alkoxy ketone via oxidative dehydrogenation with H_2O_2. The oxidative dehydrogenation activity of **2** for converting alcohols to carbonyls was confirmed by the finding that using cyclooctanol [Cy_8(OH)] as substrate led to cyclooctanone [Cy_8(=O)] as the sole product in 50% yield at 24 h (Table 3, entry 13). *cis*-1,2-Cyclooctanediol [$Cy_8(OH)_2$] was not present in measurable amounts in the reaction of Cy_8 in the presence of **2**/H_2O_2/EtOH, although its formation via acid-catalysed hydrolysis of the epoxide cannot be completely excluded since water was added together with H_2O_2. With $Cy_8(OH)_2$ as substrate, the catalytic reaction was very fast (100% conversion at 24 h, entry 15), indicating that the diol is a very reactive intermediate when compared to Cy_8O; without catalyst, the diol conversion was 99% (entry 16). Catalyst **2** with the diol (entry 15) led to Cy_8(OH)(OEt) and Cy_8(=O)(OEt) in 5% and 52% yield, respectively, together with a 28% yield of 2-hydroxycyclooctanone [Cy_8(=O)OH] and a 15% yield of 1,2-cyclooctanedione [$Cy_8(=O)_2$] (path B in Scheme 3). Hence, the diol, once formed, may undergo etherification with EtOH to give the alkoxy products. The ketones $Cy_8(=O)_2$ and Cy_8(=O)OH may be formed via oxidative dehydrogenation of the diol with H_2O_2. From these results one cannot fully exclude the possibility of the diol being an intermediate in the reaction of the olefin to the alkoxy products in H_2O_2/EtOH. Nevertheless, since $Cy_8(=O)_2$ and Cy_8(=O)OH were not present in measurable amounts in the catalytic system **2**/Cy_8/H_2O_2/EtOH (Table 3, entries 5-6), the epoxide alcoholysis route (path A) seems to be more important.

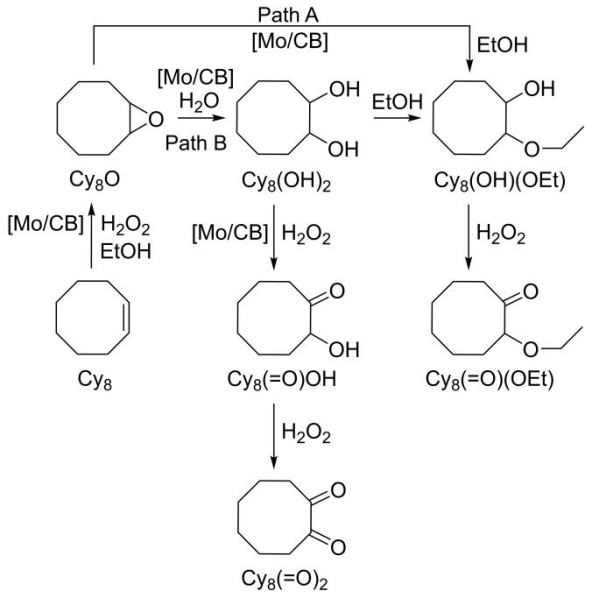

Scheme 3 One-pot conversion of cyclooctene in H_2O_2/EtOH to alkoxy alcohol and alkoxy ketone products; a mechanistic proposal involving hydrolysis and alcoholysis.

One-pot conversion of other olefins to alkoxy products

The reaction of Cy_6 gave 2-ethoxycyclohexanol [$Cy_6(OH)(OEt)$] as the main product in 60% yield at 64% conversion (24 h), while the diol $Cy_6(OH)_2$ was formed in 4% yield (Table 4). These results are interesting in that the alkoxy product was the main product in a one-pot strategy at the lower temperature of 70 °C. The absence of the alkoxy ketone product suggests that the oxidative dehydrogenation of $Cy_6(OH)(OEt)$ is demanding. In support of this supposition, the catalytic reaction of cyclohexanol [$Cy_6(OH)$] with H_2O_2/EtOH in the presence of **2** only resulted in 12% conversion after 24 h. Moreover, a comparison of the results for the substrates $Cy_8(OH)$ (Table 3, entry 13) and $Cy_6(OH)$ (Table 4) indicates that the latter is less prone to catalytic oxidative dehydrogenation. Although the epoxide Cy_6O was not present in measurable amounts with Cy_6 as substrate, it may be an intermediate in the formation of the diol and alkoxy products, as proposed in Scheme 3 for Cy_8. Accordingly, Cy_6O was found to be a very reactive substrate with **2**/H_2O_2/EtOH, giving the diol and alkoxy alcohol in 8% and 92% yield, respectively, after 24 h (Table 4).

Table 4 Catalytic results for the oxidation of cyclohexyl substrates and styrene with H_2O_2 in the presence of **2** using ethanol as solvent[a]

Substrate	Product	*T* (°C)	*t* (h)	Conversion (%)	Selectivity (%)
Cy_6	$Cy_6(OH)_2$	70	24	64	7
	$Cy_6(OH)(OEt)$				93
Cy_6O	$Cy_6(OH)_2$	70	24	100	8
	$Cy_6(OH)(OEt)$				92
$Cy_6(OH)$	$Cy_6(=O)$	70	24	12	100
Sty	BA	70	24	57	26
	StyO				9
	Ph(COOEt)				5
	$Sty(OH)_2$				58

[a] Reaction conditions: Molar ratio Mo:Substrate:H_2O_2 = 1:100:152.

There are very few reports describing the reaction Cy_6/H_2O_2 in alcohol medium in the presence of molybdenum(VI) catalysts without a cocatalyst, where alkoxy products were formed. For the reaction Cy_6/H_2O_2/MeOH at 60 °C in the presence of the homogeneous catalyst [$Mo(O)(O_2)_2(H_2O)_n$], Carrasco *et al.* found that the epoxide Cy_6O was formed in trace amounts, while the main products were the diol and alkoxy alcohol (12 and 87% selectivity at 65% conversion, 18 h), somewhat in parallel with that observed for **2**.[31]

With Sty as substrate, **2** led mainly to styrene glycol [$Sty(OH)_2$] (58% selectivity at 57% conversion); other products included StyO, BA and ethyl benzoate (Ph(COOEt)) formed in 5, 15 and 3% yield, respectively (Table 4). The corresponding alkoxy alcohol product was not present in measurable amounts. The results somewhat parallel those reported by Biradar *et al.* for Sty/H_2O_2/BuOH in the presence of the complex [$CpMo(CO)_3(C{\equiv}CPh)$] (0.2 mol%) in that the main product was the diol (82% selectivity at 95% conversion, 65 °C/10 h), and other reaction products included BA.[32] The diol may be formed via acid-catalysed hydrolysis of the epoxide in a manner similar to that represented in Scheme 3.

Catalyst reuse

With MeCN or EtOH as solvent, the reactions of Cy_8 with H_2O_2 in the presence of **2** always led to biphasic solid-liquid mixtures after 24 h batch runs. Solids were recovered for reuse by centrifugation, washing with acetone, and drying. Compound **2** was reused for four consecutive batch runs of the reaction Cy_8/H_2O_2/MeCN and two consecutive batch runs of the reaction Cy_8/H_2O_2/EtOH at 70 °C for 24 h. For MeCN, Cy_8 conversion decreased from run 1 to run 2, and to a lower extent from run 2 up to run 4 (Fig. 5). In the EtOH medium, partial loss of activity was observed from the first to the second run (Fig. 5).

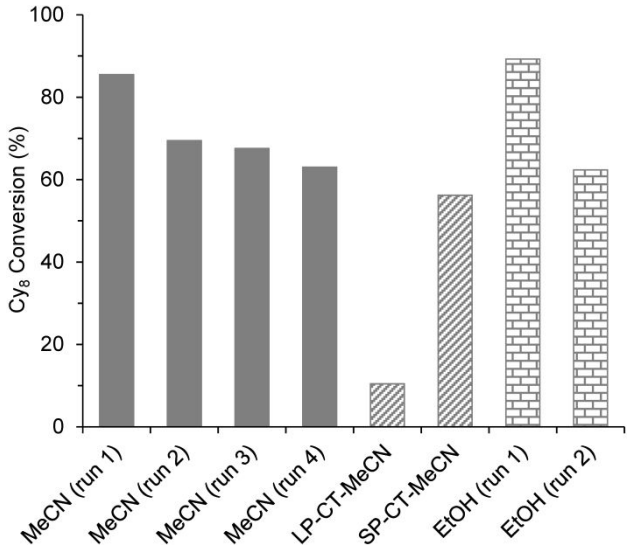

Fig. 5 Reaction of Cy_8 at 70 °C for 24 h using **2**/H_2O_2/MeCN (catalyst reuse for four runs), the liquid (LP) or solid (SP) phases from the contact test (CT) for **2** in MeCN medium, and **2**/H_2O_2/EtOH (catalyst reuse for two runs).

A contact test (CT) was carried out for **2** by mixing it with H_2O_2/MeCN (without substrate) at 70 °C for 24 h. The resultant liquid and solid phases (denoted LP-CT-MeCN and SP-CT-MeCN, respectively) were separated and tested for the reaction Cy_8/H_2O_2/MeCN at 70 °C for 24 h. The liquid phase LP-CT-MeCN did not lead to significant olefin conversion (10% at 24 h), while the solid phase SP-CT-MeCN led to similar catalytic results to those for run 2 (Fig. 5). These results suggest that the catalytic reaction occurred essentially in heterogeneous phase.

The solids recovered after each batch run were characterised by attenuated total reflectance (ATR) FT-IR spectroscopy, PXRD and SEM (with EDS elemental mapping). Representative results are shown in the ESI† for the reactions **2**/Cy_8/H_2O_2/MeCN, **2**/Sty/H_2O_2/MeCN and **2**/Sty/H_2O_2/EtOH performed at 70 °C, and **2**/Cy_8/H_2O_2/EtOH performed at 90 °C. The ATR FT-IR spectra (Fig. S3), PXRD patterns (Fig. S4) and SEM images (Fig. S5) of the solids recovered after the first run of each reaction system were similar, but displayed differences when compared with those for **2**. No further significant alterations were observed for the solids recovered after the runs 2 and 3. Hence, structural features of **2** changed during the first contact with the reaction medium and then remained similar, which correlates with the catalytic activity in consecutive batch runs for the reaction **2**/Cy_8/H_2O_2/MeCN. Regarding the FT-IR spectra,

the major change between **2** and the recovered solids was the weakening (or complete loss) of the ν_{asym}(Mo=O) absorption band at 915 cm^{-1} (Fig. S3). This was accompanied by the appearance of some very weak bands between 850 and 900 cm^{-1}, especially one at 888 cm^{-1}, which may be due to peroxide ligands [ν(O–O)] formed via the coordination of H_2O_2 to molybdenum centres. The catalytic role of peroxomolybdenum(VI) species that may be formed in (dioxomolybdenum/H_2O_2)-catalysed olefin epoxidation systems is well-established, based on studies of different research groups worldwide.[33] Several mechanistic hypotheses have been put forward (mainly based on gas-phase density functional theory) for olefin epoxidation with hydroperoxides in the presence of oxoperoxomolybdenum species; reaction mechanisms may involve O-atom transfer from a η^2-O_2 peroxo ligand[33c,34] or a hydroperoxo ligand[33d,34a,35] to the olefin (which may or may not be coordinated to the metal centre).

The PXRD patterns of all the recovered solids indicated that the crystalline structure of **2** underwent a reorganisation under the different reaction conditions to give a CB[6] crystal packing arrangement equivalent to that present in as-synthesized CB[6] (Fig. S4). No marked change in morphology occurred according to SEM (Fig. S5). EDS elemental mappings of **2** and all the recovered solids revealed uniform distributions of Mo, N and O (Fig. S5). The EDS-determined N/Mo atomic ratio was 9.4 for **2**, and 12.7 for the solid recovered after run 1 of the reaction **2**/Cy_8/H_2O_2/MeCN performed at 70 °C. This may point to slight metal leaching during the first catalytic run using MeCN as solvent. However, after run 1, the N/Mo ratio remained roughly constant (less than 5% variance), which correlates with the steady catalytic activity after run 1. These results, together with those for the contact test, suggest that any metal species leached into solution had negligible catalytic contribution. With ethanol as the solvent (**2**/Cy_8/H_2O_2/EtOH), the N/Mo ratio for the used catalyst was 9.2, similar to that for the original catalyst, suggesting good stability towards metal leaching in the alcohol media used for one-pot conversions. The understanding of the behaviour of these types of crystalline supramolecular compounds for solid-liquid catalysis is important, being a subject of investigation in our laboratories, with special focus on the structural and morphological stability.

Conclusions

In conclusion, we have demonstrated that the macrocyclic cavitand cucurbit[6]uril can be used for the solid-state isolation of the complex $[MoO_2Cl_2(H_2O)_2]$ from hydrochloric acid solution. In the resultant crystalline supramolecular compound (**2**), the diaqua complexes are embedded between barrel-shaped hydrogen-bonded entities, {CB[6]·10(H_2O)}, which are arranged in layers. Although the activity of compound **2** for the catalytic oxidation of *cis*-cyclooctene is moderate, it has the advantage of using H_2O_2 as oxidant, and the selectivity towards the epoxide is very high (90-100%) for reaction temperatures up to 70 °C and different solvents. Another advantage is that the reaction outcome with an alcohol as solvent can be shifted towards the formation of alkoxy ketone and alkoxy alcohol products by adopting a one-pot strategy comprising an oxidation stage at 70 °C (with H_2O_2) followed by an acid-catalysed stage at 90 °C. To the best of our knowledge, this is the first report of the one-pot Mo-catalysed oxidation of an alkene with H_2O_2 in alcohol medium to give alkoxy ketone products. While the reaction of cyclohexene in MeCN gave the diol with 100% selectivity, the reaction in ethanol gave 2-ethoxycyclohexanol as the main product (93% selectivity) even at the lower temperature of 70 °C. Mechanistic studies using the probable cyclooctyl and cyclohexyl intermediates as substrates indicate that epoxide alcoholysis is the most important pathway for the formation of the alkoxy products. The CB[6]/Mo^{VI} catalyst presented steady performance after run 2, which correlated with the similar characterisation results of the catalyst recovered from run 2 onwards. Considering the known effectiveness of molybdenum(VI) catalysts for olefin epoxidation, the data presented here encourage a more comprehensive study of Mo^{VI}-containing supramolecular compounds as multifunctional catalysts for the target integrated catalytic reaction systems.

Experimental

Synthesis of adduct $2[MoO_2Cl_2(H_2O)_2]\cdot(C_{36}H_{36}N_{24}O_{12})\cdot xH_2O\cdot yHCl\cdot z(CH_3COCH_3)$ (2)

A suspension of MoO_3 (1.20 g, 8.30 mmol) and 6 M HCl (10 mL) was heated near the boiling point for 2 h until most of the MoO_3 was dissolved, and then cooled to room temperature and filtered. A portion (2 mL) of the solution containing the complex $[MoO_2Cl_2(H_2O)_2]$ was slowly added to a solution of CB[6] (0.4 g, 0.32 mmol) in 3.8 M HCl (17.2 mL). The mixture was stirred for 2 h at room temperature during which time a colourless or very pale yellow solid precipitated. After allowing the mixture to stand for one day, the precipitate was filtered and vacuum-dried. Yield: 0.17 g, 29% (based on CB[6]). Anal. Calcd for $2[MoO_2Cl_2(H_2O)_2]\cdot(C_{36}H_{36}N_{24}O_{12})\cdot 15H_2O\cdot 1.5HCl\cdot 0.6(CH_3COCH_3)$ (1826.3): C, 24.86; H, 4.37; N, 18.41. Found: C, 25.07; H, 4.11; N 18.52. TGA revealed a weight loss of 20.6% up to 150 °C [calcd for loss of $19H_2O$ and $0.6(CH_3COCH_3)$: 20.7%]. After isolating the precipitate, the mother liquor was left to stand, which led to the formation of yellow single crystals suitable for XRD.

Catalytic oxidation experiments

The catalytic experiments were performed in tubular glass pear-shaped reactors, equipped with a PTFE-coated magnetic stirring bar and a valve, under batch operation mode. Typically, for the oxidation reactions, the reagents were loaded into the reactor in the molar proportion 1:100:152 (Mo:substrate:oxidant); specifically, 18 μmol Mo, 1.8 mmol substrate, 2.75 mmol H_2O_2 and 2 mL of a solvent. The loaded reactor was immersed in a thermostatically controlled oil bath heated at 70 °C (stirring rate of 1000 rpm to avoid mass transfer limitations) which was taken as the instant that the reaction began (zero time).

Catalyst stability studies involved the reuse of the recovered catalyst, a contact test, and characterisation of the used catalysts. Compound **2** was used for four consecutive catalytic

batch runs, under similar reaction conditions (Cy_8/H_2O_2/MeCN, 70 °C, 24 h). Catalyst recovery involved separation of the solid from the reaction mixture by centrifugation (ca. 3500 rpm for 5 min), thoroughly washing with acetone, drying at room temperature overnight and then under vacuum at 50 °C for 1 h.

The CT was carried out to check for the presence of leached active metal species in the liquid phase. First, the original catalyst was contacted with MeCN/H_2O_2 at 70 °C/24 h under similar conditions to those used for a normal catalytic test, but without substrate. Subsequently, the mixture was cooled to ambient temperature, centrifuged (3500 rpm), and filtered through a 0.2 μm PTFE membrane to separate the solid and liquid phases. The liquid phase (LP) obtained from the CT (LP-CT-MeCN) was transferred to a separate clean reactor and the substrate Cy_8 was then added to give the same initial concentration (0.79 M) as that used for a normal catalytic test. Afterwards, the homogeneous reaction mixture was heated at 70 °C for 24 h (1000 rpm). The undissolved solid obtained from the CT was washed, dried overnight under atmospheric conditions and then under vacuum for 1 h at 50 °C, giving SP-CT-MeCN.

The reactors were cooled to ambient temperature in cold water before opening and suitable work-up procedures. The analyses were always carried out for freshly prepared samples. Individual experiments were performed for each reaction of 24 h (experimental error of ca. 5%). The evolution of the catalytic reactions was monitored by GC using a Varian 3800 instrument equipped with an Agilent J&W VF-5ms capillary column (30 m × 0.25 mm × 0.25 μm), a flame ionisation detector, H_2 as the carrier gas and undecane as internal standard. The reaction products were identified by GC-MS with a Trace GC Ultra 2000 instrument (Thermo Quest CE instruments) equipped with a DSQ II (Thermo Scientific) mass selective detector and an Agilent J&W DB-1 capillary column (30 m × 0.25 mm × 0.25 μm). He was used as the carrier gas and the commercial databases Wiley 6 and NIST Mainlib and Replib were used. The mass spectral data for selected products are given in the ESI†.

Conflicts of interest

There are no conflicts to declare.

Acknowledgements

We acknowledge the support of CICECO - Aveiro Institute of Materials [FCT (Fundação para a Ciência e a Tecnologia) Ref. UID/CTM/50011/2019], REQUIMTE-LAQV (UID/QUI/50006/2013 - POCI/01/0145/FEDER/007265), Centre of Marine Sciences - CCMAR (UID/Multi/04326/2019), and the CENTRO 2020 Regional Operational Programme (Project CENTRO-01-0145-FEDER-028031; PTDC/QUI-QOR/28031/2017), co-financed by national funds through the FCT/MEC and the European Union (EU) through the European Regional Development Fund under the Portugal 2020 Partnership Agreement. The FCT and the EU are acknowledged for a Ph.D. grant to L.S.N. (PD/BD/109666/2015). The positions held by M.M.A and A.C.G. were funded by national funds (OE), through FCT, I.P., in the scope of the framework contract foreseen in the numbers 4, 5 and 6 of article 23 of the Decree-Law 57/2016 of 29 August, changed by Law 57/2017 of 19 July.

Notes and references

1 *(a)* J. J. Berzelius, *Ann. Phys. Lpz.*, 1826, **46**, 381; *(b)* R. Colton and I. B. Tomkins, *Aust. J. Chem.*, 1965, **18**, 447-452.
2 *(a)* K. Jeyakumar and D. K. Chand, *J. Chem. Sci.*, 2009, **121**, 111-123; *(b)* S. C. A. Sousa, I. Cabrita and A. C. Fernandes, *Chem. Soc. Rev.*, 2012, **41**, 5641-5653; *(c)* R. G. de Noronha and A. C. Fernandes, *Curr. Org. Chem.*, 2012, **16**, 33-64.
3 L. O. Atovmyan, Z. G. Aliev and B. M. Tarakanov, *Zh. Strukt. Khim.*, 1968, **9**, 1097-1098; L. O. Atovmyan, Z. G. Aliev and B. M. Tarakanov, *J. Struct. Chem.*, 1969, **9**, 985-986.
4 L. O. Atovmyan and Z. G. Aliev, *Zh. Strukt. Khim.*, 1971, **12**, 732-734; L. O. Atovmyan and Z.G. Aliev, *J. Struct. Chem.*, 1971, **12**, 668-669.
5 J. M. Coddington and M. J. Taylor, *J. Chem. Soc., Dalton Trans.*, 1990, 41-47.
6 F. J. Arnaiz, R. Aguado, J. Sanz-Aparicio and M. Martinez-Ripoll, *Polyhedron*, 1994, **13**, 2745-2749.
7 (a) M. J. Taylor, C. E. F. Rickard and L. A. Kloo, *J. Chem. Soc., Dalton Trans.*, 1998, 3195-3198; *(b)* W. Levason, R. Ratnani, G. Reid and M. Webster, *Inorg. Chim. Acta*, 2006, **359**, 4627-4630.
8 B. Kamenar and M. Penavić, *Acta Cryst.*, 1976, **B32**, 3323-3324.
9 M. J. Taylor, W. Jirong and C. E. F. Rickard, *Polyhedron*, 1993, **12**, 1433-1435.
10 Y. Luan, G. Wang, R. L. Luck and M. Yang, *Eur. J. Inorg. Chem.*, 2007, 1215-1218.
11 J. S. Costa, C. M. Markus, I. Mutikainen, P. Gamez and J. Reedijk, *Inorg. Chim. Acta*, 2010, **363**, 2046-2050.
12 *(a)* E. Masson, X. Ling, R. Joseph, L. Kyeremeh-Mensah and X. Lu, *RSC Adv.*, 2012, **2**, 1213-1247; *(b)* K. I. Assaf and W. M. Nau, *Chem. Soc. Rev.*, 2015, **44**, 394-418; *(c)* S. J. Barrow, S. Kasera, M. J. Rowland, J. del Barrio and O. A. Scherman, *Chem. Rev.*, 2015, **115**, 12320-12406.
13 *(a)* J. Lü, J.-X. Lin, M.-N. Cao and R. Cao, *Coord. Chem. Rev.*, 2013, **257**, 1334-1356; *(b)* X.-L. Ni, X. Xiao, H. Cong, Q.-J. Zhu, S.-F. Xue and Z. Tao, *Acc. Chem. Res.*, 2014, **47**, 1386-1395; *(c)* X.-L. Ni, X. Xiao, H. Cong, L.-L. Liang, K. Cheng, X.-J. Cheng, N.-N. Ji, Q.-J. Zhu, S.-F. Xue and Z. Tao, *Chem. Soc. Rev.*, 2013, **42**, 9480-9508.
14 *(a)* E. A. Kovalenko, D. Y. Naumov and V. P. Fedin, *Polyhedron*, 2018, **144**, 158-165, and references cited therein; *(b)* O. A. Gerasko, E. A. Mainicheva, M. I. Naumova, O. P. Yurjeva, A. Alberola, C. Vicent, R. Llusar and V. P. Fedin, *Eur. J. Inorg. Chem.*, 2008, 416-424, and references cited therein; *(c)* D. G. Samsonenko, A. V. Virovets, A. A. Sharonova, V. P. Fedin and D. Fenske, *Russ. Chem. Bull. Int. Ed.*, 2001, **50**, 494-496; *(d)* O. A. Gerasko, E. A. Mainicheva, D. Y. Naumov and V. P. Fedin, *Russ. Chem. Bull. Int. Ed.*, 2007, **56**, 1972-1977.
15 F. H. Allen and W. D. S. Motherwell, *Acta Crystallogr.,* Sect. *B: Struct. Sci.*, 2002, **58**, 407-422.
16 F. H. Allen, *Acta Crystallogr., Sect. B: Struct. Sci.*, 2002, **58**, 380-388.
17 Y. Luan, G. Wang, R. L. Luck, Y. N. Wang, H. Xiao and H. J. Ding, *Chem. Lett.*, 2008, **37**, 1144-1145.
18 B. D. Wagner and A. I. Macrae, *J. Phys. Chem. B*, 1999, **103**, 10114-10119.
19 J. G. Smith, *Synthesis*, 1984, 629-656.
20 *(a)* S. B. Khomane, D. S. Doke, M. K. Dongare, S. B. Halligudi and S. B. Umbarkar, *Appl. Catal. A: Gen.*, 2017, **531**, 45-51; *(b)* D. Biswal, N. R. Pramanik, S. Chakrabarti, M. G. B. Drew, B.

Sarkar, M. R. Maurya, S. K. Mukherjee and P. Chowdhury, *New J. Chem.*, 2017, **41**, 4116-4137.
21 *(a)* M. E. Conolly, F. Kersting and C. T. Dollery, *Prog. Cardiovas. Dis.*, 1976, **19**, 203-234; *(b)* J. Joossens, P. Van der Veken, A. M. Lambeir, K. Augustyns and A. Haemers, *J. Med. Chem.*, 2004, **47**, 2411-2413; *(c)* P. Stead, H. Marley, M. Mahmoudian, G. Webb, D. Noble, Y. T. Ip, E. Piga, T. Rossi, S. Roberts and M. J. Dawson, *Tetrahedron: Asymmetry*, 1996, **7**, 2247-2250.
22 P. G. M. Wuts and T. W. Greene, in: P. G. M. Wuts and T. W. Greene (Eds.), Greene's Protective Groups in Organic Synthesis, John Wiley & Sons, Inc., New Jersey, USA, 2006.
23 E. J. King, in: A. K. Covington and T. Dickson (Eds.), Physical Chemistry of Organic Solvent Systems, Springer, London, Plenum Publishing Company Ltd., 1973, Chapter 3.
24 *(a)* S. Roy, Saswati, S. Lima, S. Dhaka, M. R. Maurya, R. Acharyya, C. Eagle and R. Dinda, *Inorg. Chim. Acta*, 2018, **474**, 134-143; *(b)* M. R. Maurya and N. Kumar, *J. Mol. Catal. A: Chem.*, 2015, **406**, 204-212.
25 S. K. Maiti, S. Dinda and R. Bhattacharyya, *Tetrahedron Lett.*, 2008, **49**, 6205-6208.
26 V. Hulea and E. Dumitriu, *Appl. Catal. A: Gen.*, 2004, **277**, 99-106.
27 A. Patel and S. Pathan, *Ind. Eng. Chem. Res.*, 2012, **51**, 732-740.
28 M. R. Maurya, A. Arya, P. Adão and J. C. Pessoa, *Appl. Catal. A: Gen.*, 2008, **351**, 239-252.
29 X. Huang, W. Guo, G. Wang, M. Yang, Q. Wang, X. Zhang, Y. Feng, Z. Shi and C. Li, *Mater. Chem. Phys.,* 2012, **135**, 985-990.
30 M. Hashimoto, K. Itoh, K. Y. Lee and M. Misono, *Top. Catal.*, 2001, **15**, 265-271.
31 C. J. Carrasco, F. Montilla, E. Álvarez, M. Herbert and A. Galindo, *Polyhedron*, 2013, **54**, 123-130.
32 A. V. Biradar, B. R. Sathe, S. B. Umbarkar and M. K. Dongare, *J. Mol. Catal. A: Chem.*, 2008, **285**, 111-119.
33 *(a)* S. Berski, F. R. Sensato, V. Polo, J. Andrés and V. S. Safont, *J. Phys. Chem. A*, 2011, **115**, 514-522; *(b)* M. Herbert, F. Montilla, E. Álvarez and A. Galindo, *Dalton Trans.*, 2012, **41**, 6942-6956; *(c)* M. Herbert, E. Álvarez, D. J. Cole-Hamilton, F. Montilla and A. Galindo, *Chem. Commun.*, 2010, **46**, 5933-5935; *(d)* M. J. Calhorda and P. J. Costa, *Curr. Org. Chem.*, 2012, **16**, 65-72.
34 *(a)* V. Yudanov, *J. Struct. Chem., Supplement*, 2007, **48**, S111-S124; *(b)* M. Drees, S. A. Hauser, M. Cokoja and F. E. Kühn, *J. Organomet. Chem.*, 2013, **748**, 36-45.
35 M. Herbert, F. Montilla, E. Álvarez and A. Galindo, *Dalton Trans.*, 2012, **41**, 6942-6956.